

---

---

# Evaluation of an Automated Module Synthesis and a Sterile Cold Kit–Based Preparation of $^{68}\text{Ga}$ -PSMA-11 in Patients with Prostate Cancer

Letizia Calderoni<sup>1</sup>, Andrea Farolfi<sup>1</sup>, Davide Pianori<sup>2</sup>, Elisa Maietti<sup>2</sup>, Veronica Cabitza<sup>3</sup>, Alessandro Lambertini<sup>1</sup>, Giacomo Ricci<sup>1</sup>, Silvi Telo<sup>1</sup>, Filippo Lodi<sup>3</sup>, Paolo Castellucci<sup>1</sup>, and Stefano Fanti<sup>1</sup>

<sup>1</sup>Nuclear Medicine, St. Orsola Hospital, University of Bologna, Bologna, Italy; <sup>2</sup>Department of Biomedical and Neuromotor Sciences, University of Bologna, Bologna, Italy; and <sup>3</sup>PET Radiopharmacy Unit, St. Orsola Hospital, University of Bologna, Bologna, Italy

$^{68}\text{Ga}$ -labeled urea-based inhibitors of the prostate-specific membrane antigen (PSMA), such as  $^{68}\text{Ga}$ -PSMA-11, are promising small molecules for targeting prostate cancer (PCa). Although this radiopharmaceutical was produced mostly by means of manual synthesis and automated synthesis modules, a sterile cold kit was recently introduced. The aim of our study was to evaluate the image quality of  $^{68}\text{Ga}$ -PSMA-11 PET/CT (PSMA-PET) in a population of PCa patients after the injection of comparable activities of  $^{68}\text{Ga}$ -PSMA-11 obtained with the 2 different synthetic procedures. A secondary aim was to identify secondary factors that may have an impact on image quality and, thus, final interpretation. **Methods:** Two different groups of 100 consecutive PCa patients who underwent PSMA-PET were included in the study. The first group of patients was imaged with  $^{68}\text{Ga}$ -PSMA-11 obtained using synthesis modules, whereas the second group's tracer activity was synthesized using a sterile cold kit. All PET images were independently reviewed by 2 nuclear medicine diagnosticians with at least 2 y of experience in PSMA-based imaging and unaware of the patients' clinical history. The 2 reviewers independently rated the quality of each PSMA-PET scan using a 3-point Likert-type scale. In cases of discordance, the operators together reviewed the images and reached a consensus. Performance was evaluated on the basis of the expected biodistribution, lesion detection rate, and physiologic background uptake. **Results:** Overall, 104 of 200 (52%) PSMA-PET scans were positive for PCa-related findings. No significant differences in image quality between cold kits and synthesis modules were found ( $P = 0.13$ ), although a higher proportion of images was rated as excellent by the observers for kits than for modules (45% vs. 34%). Furthermore, after image quality had been dichotomized as excellent or not excellent, multivariate regression analysis found several factors to be significantly associated with a not-excellent quality: an increase in patient age (+5 y: odds ratio [OR], 1.40; 95% confidence interval [CI], 1.12–1.75), an increase in patient weight (+5 kg: OR, 1.89; 95% CI, 1.53–2.32), an increase in  $^{68}\text{Ga}$ -PSMA-11 uptake time (+10 min: OR, 1.45; 95% CI, 1.08–1.96), and a decrease in injected activity (–10 MBq: OR, 1.28; 95% CI, 1.07–1.52). **Conclusion:** No significant differences were identified between the 2 groups of patients undergoing PSMA-PET; therefore, we were not able to ascertain any significant influences of tracer production methodology on final scan quality. However, increased patient age, increased patient weight, decreased injected activity, and increased  $^{68}\text{Ga}$ -PSMA-11 uptake time were significantly associated with an overall poorer image quality.

**Key Words:** PSMA; sterile cold kit; automated synthesis module; prostate cancer; PET/CT

**J Nucl Med 2020; 61:716–722**  
DOI: 10.2967/jnumed.119.231605

**P**rostate cancer (PCa) has the second highest incidence and is the fifth highest cause of cancer-related death among men (1). Accurate identification of PCa represents a major challenge among the urologic community at all different disease stages, namely primary staging, biochemical recurrence, and castration resistance. Conventional imaging modalities for the detection of PCa include MRI, bone scintigraphy, CT, and PET. In recent years, the introduction of a new class of small-molecule prostate-specific membrane antigen (PSMA) inhibitor radiotracers has shown promising results for imaging of PCa. PSMA is a glutamate carboxypeptidase II, a membrane-bound metallopeptidase present at high levels on PCa cells (2). Despite the name, PSMA is not specific to the prostate gland and is expressed in several normal tissues (duodenal mucosa, salivary glands, renal tubular cells) and neoplastic tissues (renal cell carcinoma, tumoral neovasculature). PSMA-ligand PET/CT reveals the expression of PSMA and detects PCa metastases with accuracy superior to conventional imaging (3). Compared with other imaging techniques, PSMA-ligand PET/CT has an improved detection rate for smaller lesions, and PSMA ligands may be able to identify nodal or distant metastatic disease at earlier stages and in lower ranges of PSA than other PET radiotracers (4). Several molecular PSMA-targeted tracers have been investigated in both PET and SPECT imaging, and for PET imaging, a variety of PSMA ligands has been introduced into clinical practice, bound with different radioisotopes as shown in Table 1. Many data have been presented in the literature, especially for PSMA-11, and some for PSMA imaging and therapy, labeled with  $^{68}\text{Ga}$  (5–8). Recently  $^{18}\text{F}$ -labeled compounds have been proposed for PSMA imaging, such as  $^{18}\text{F}$ -DCFBC,  $^{18}\text{F}$ -DCFPL, and  $^{18}\text{F}$ -PSMA-1007, for their potentially easier production and distribution logistics (9–11). To date, the  $^{68}\text{Ga}$ -labeled PSMA inhibitor Glu-NH-CO-NH-Lys(Ahx)-HBED-CC ( $^{68}\text{Ga}$ -PSMA-11) is the most used radioligand for PET/CT (12). Nowadays, a simplified production and simpler distribution logistics assume great importance, since  $^{68}\text{Ga}$ -PSMA-11 PET/CT (PSMA-PET) imaging is in increasing use. Furthermore, several methods of labeling and preparation have been introduced for the production of  $^{68}\text{Ga}$ -PSMA-11 ligands (13). Since

---

Received May 29, 2019; revision accepted Sep. 16, 2019.  
For correspondence or reprints contact: Andrea Farolfi, Nuclear Medicine, St. Orsola University Hospital, Via Albertoni 15, Bologna, Italy.  
E-mail: andrea.farolfi5@studio.unibo.it  
Published online Oct. 10, 2019.  
COPYRIGHT © 2020 by the Society of Nuclear Medicine and Molecular Imaging.

**TABLE 1**  
Overview of Several Molecular PSMA-Targeted Agents and Radioisotopes

Radioisotope	PSMA ligand	Description
<sup>123</sup> I <sup>99m</sup> Tc	MIP-1072 and MIP-1095 MIP-1404 and MIP-1405	First agents for SPECT imaging
<sup>18</sup> F <sup>68</sup> Ga	DCFBC PSMA-11	First agents for PET imaging
<sup>68</sup> Ga, <sup>177</sup> Lu, <sup>255</sup> Ac <sup>68</sup> Ga, <sup>177</sup> Lu, <sup>111</sup> In	PSMA-617 PSMA imaging and therapy (better known as PSMA I&T)	Theranostic ligands
<sup>18</sup> F <sup>18</sup> F	<sup>18</sup> F-DCFPyL <sup>18</sup> F-PSMA-1007	Second generation of tracers labeled with <sup>18</sup> F

the half-life of <sup>68</sup>Ga is relatively short (68 min), reducing production time may significantly increase the available tracing activity in each elution charge. This effect, in turn, may be beneficial to a high-volume PET imaging center, as well as decreasing the costs of each examination. Although <sup>68</sup>Ga-PSMA-11 ligands are commonly produced via automated synthesis modules, and sometimes by manual

synthesis processes, which are time-consuming, a sterile cold kit for <sup>68</sup>Ga-PSMA-11 production was recently introduced. In this retrospective study, we investigated the impact of 2 different <sup>68</sup>Ga-PSMA-11 synthetic procedures on PET/CT image quality. We also investigated, as secondary aims, the roles played by external factors, including patient age, patient weight, patient body mass index (BMI), injected activity, uptake time, and image acquisition methodology, in influencing image quality.

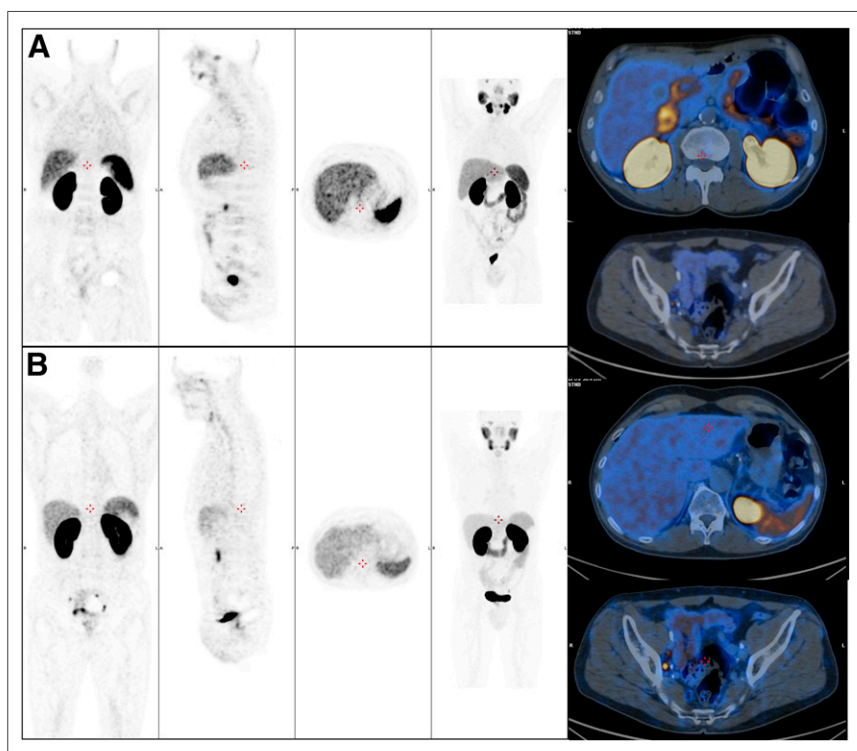


**FIGURE 1.** Comparison of 2 <sup>68</sup>Ga-PSMA-11 PET/CT acquisitions rated as good quality using different production procedures. (A) <sup>68</sup>Ga-PSMA-11 synthesized with sterile cold kit, for 68-y-old patient with extracapsular PCa at time of diagnosis. Initial PSA was 6.1 ng/mL. Gleason score was 7 (4 + 3). External-beam radiation therapy was performed in 2012, and a combination of anti-androgen and LH-RH analog was given for 2 y, until 2014. Biochemical recurrence occurred during 2015. PSA doubling time was less than 6 mo. PSA at time of PET/CT was 2.5 ng/mL. From left to right are shown coronal PET, sagittal PET, axial PET, maximum-intensity projection, PET/CT of abdomen (top), and PET/CT of pelvis (bottom). (B) <sup>68</sup>Ga-PSMA-11 synthesized with automated module, for 72-y-old patient with PCa. Gleason score was 8 (4 + 4). Initial PSA was 6.9 ng/mL. Radical prostatectomy with nerve sparing and pelvic lymphadenectomy were performed in 2017. Stage was pT3a pN1. PSA persisted for 2 mo after surgery. PSA at time of PET/CT was 1.19 ng/mL. From left to right are shown coronal PET, sagittal PET, axial PET, maximum-intensity projection, PET/CT of abdomen (top), and PET/CT of pelvis (bottom).

## MATERIALS AND METHODS

### Patient Population

PSMA-PET imaging is an option offered at our institution to PCa patients within the framework of an investigational new drug trial (PSMA PROSTATA; EudraCT 2015 004589 27 OsSC). In our retrospective single-center study, we enrolled 2 groups of consecutive PCa patients (100 patients each) who underwent PSMA-PET: the first group between April and June 2017 and the second one between October and December 2017. No patients had a known second primary cancer. The institutional Ethics Committee approved this retrospective study. All participants included in the study gave written informed consent after being appropriately informed of the purpose of the study.

### <sup>68</sup>Ga-PSMA-11 Preparation

**Synthesis Module.** In the first cohort of 100 patients, <sup>68</sup>Ga-PSMA-11 was produced by means of a synthesis module (Modular-Lab Pharm Tracer; Eckert and Ziegler) equipped with sterile single-use cassettes (C4-GA68-PSMA; Eckert and Ziegler) using the eluate of a GalliaPharm generator (1,850 MBq; Eckert and Ziegler). <sup>68</sup>Ga was eluted with 5 mL of 0.1N HCl (Eckert and Ziegler) and trapped onto a strong cation exchange column for purification. <sup>68</sup>Ga was then slowly eluted with 0.8 mL of 5N NaCl/5.5N HCl solution in a reactor with the precursor PSMA-11 (25 µg, good-manufacturing-practice grade; ABX Germany) dissolved in sodium acetate buffer (0.4 mL, pH 4.5). The labeling reaction was performed at 95°C for 5 min. The crude product was diluted with 2 mL of 0.9% NaCl and

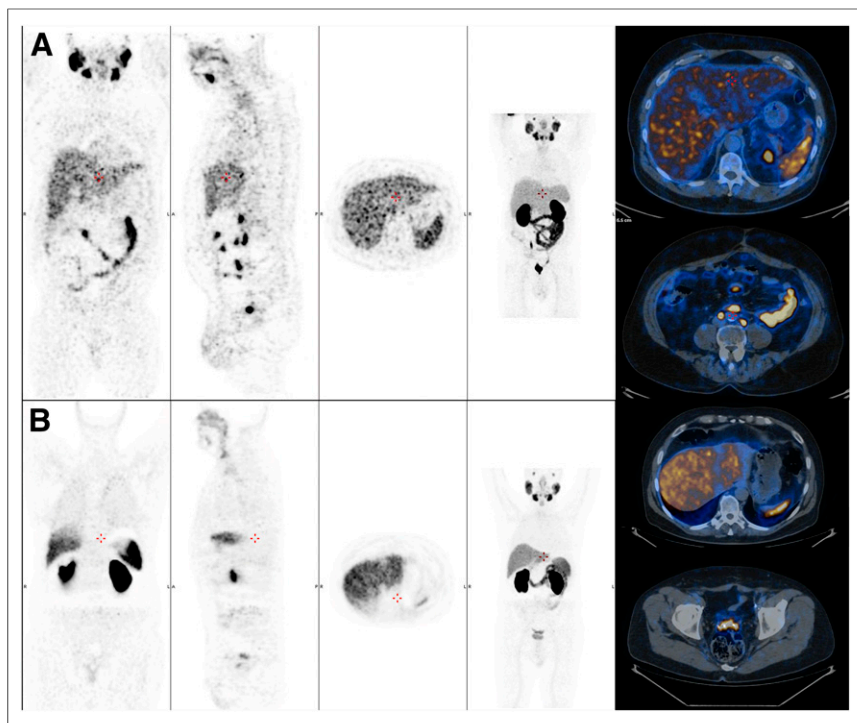


**FIGURE 2.** Comparison of 2  $^{68}\text{Ga}$ -PSMA-11 PET/CT acquisitions rated as moderate quality using different production procedures. (A)  $^{68}\text{Ga}$ -PSMA-11 synthesized with sterile cold kit, for 81-y-old patient with PCa. Gleason score was 8 (4 + 4). Patient underwent radical prostatectomy in 2009. Stage was pT4pN1 (1/10) R0. Initial PSA was 10.67. Adjuvant radiotherapy on prostate bed and pelvic lymph nodes was performed, as well as anti-androgen plus LH-RH analog. During 2016, stereotactic radiation therapy was performed on iliac lymph nodes. PSA at time of PET/CT was 1.19 ng/mL. From left to right are shown coronal PET, sagittal PET, axial PET, maximum-intensity projection, PET/CT of abdomen (top), and PET/CT of pelvis (bottom). (B)  $^{68}\text{Ga}$ -PSMA-11 synthesized with automated module, for 76-y-old patient with PCa. Gleason score was 9 (5 + 4). In 2014, radical prostatectomy and pelvic lymphadenectomy were performed. Initial PSA was 7.5 ng/mL. Stage was pT3b R+N2 (8/20) M0. External-beam radiation was performed on prostate bed. PSA at time of PET/CT was 5.92 ng/mL. From left to right are shown coronal PET, sagittal PET, axial PET, maximum-intensity projection, PET/CT of abdomen (top), and PET/CT of pelvis (bottom).

loaded onto a C18 column for purification. The product was eluted with 1 mL of ethanol, diluted with 8 mL of 0.9% NaCl, and sterilized by means of a 0.22- $\mu\text{m}$  filter.

**Cold Kit.** For the second group of patients, production runs were performed using a lyophilized sterile cold kit with PSMA-11 (ANMI SA). All necessary materials to perform the radiolabeling are provided with the kit.  $^{68}\text{Ga}$  was eluted in a vacuumed sterile vial (5 mL of 0.1N HCl, 1,850-MBq GalliaPharm generator; Eckert and Ziegler). In a second sterile vial, the lyophilized precursor PSMA-11 (25  $\mu\text{g}$ ) was reconstituted with acetate buffer. The precursor solution was then added to the elution vial, and the labeling reaction was performed within 5 min at room temperature.

**Quality Control.** The radiochemical purity of each batch was determined by a high-performance liquid chromatograph equipped with a radio-detector and an ultraviolet detector, and by thin-layer chromatography. For the high-performance liquid chromatography, the mobile phase was water with 0.1% trifluoroacetic acid (A) and acetonitrile with 0.1% trifluoroacetic acid (B), with a linear gradient of 10%–30% (B) in 10 min. The stationary phase was on a C8 column (Eclipse XDB-C8; Agilent) with a flow rate of 1.5 mL/min and a wavelength of 220 nm. For the thin-layer chromatography, the mobile phase was a 1:1 solution of ammonium acetate (77 g/L)/methanol, and the stationary phase was a silica gel plate. Ethanol content (only for the synthesis module method) was measured by

gas chromatography (capillary column, CP-Wax 52 CB; Varian). The residual  $^{68}\text{Ge}$  content was evaluated by  $\gamma$ -ray spectrometry (high-purity germanium detector). Sterility and pyrogen content were tested according to European Pharmacopoeia methods.

### PET/CT Acquisition and Image Reconstruction

PET/CT scans were performed between 48 and 114 min (mean uptake time, 73 min) after intravenous injection of  $^{68}\text{Ga}$ -PSMA-11 using a weight-tailored activity of 2 MBq/kg of body weight in a total volume of 5–10 mL. The average injected activity was 150 MBq (range, 96–225 MBq). PET images were acquired in accordance with the joint procedure guidelines of the Society of Nuclear Medicine and Molecular Imaging and the European Association of Nuclear Medicine for PCa imaging (14). Acquisitions were performed using 2 different dedicated PET/CT hybrid systems (Discovery STE and Discovery 710; GE Healthcare). All patients were positioned supine on the imaging table with their arms above their head, and the acquisition proceeded from the base of the skull to the mid thighs. PET emission images were recorded for 3 min per bed position in three-dimensional mode using the Discovery STE (122/200 patients) or the Discovery 710 (78/200 patients). All images were corrected for scatter, random coincidence events, system dead time, and decay. CT images were used for correction (120 kV, 80 mA, 0.8-s tube rotation, and 3.75-mm thickness). Attenuation-CT imaging was performed without intravenous contrast enhancement. PET images were reconstructed using a fully tridimensional iterative algorithm.

### Image Interpretation

PSMA-PET images were analyzed using a dedicated workstation equipped with a commercially available software package (Advantage Workstation 4.6; GE Healthcare) allowing simultaneous and fused reviewing of PET and CT data. Two experienced nuclear medicine specialists independently reviewed all PSMA-PET images, and in cases of disagreement the report was finalized after they had reached a consensus. Any nonphysiologic, focal areas of  $^{68}\text{Ga}$ -PSMA-11 uptake higher than the normal background were considered significant and likely sites of disease. Lesions were grouped and recorded according to the Prostate Cancer Molecular Imaging Standardized Evaluation (PROMISE) classification; in particular, criteria were separately given for imaging of the prostate bed after radical prostatectomy or after external-beam radiation therapy, for primary staging of cancer, for lymph node imaging, and for imaging of visceral bones or organs (15). Classification of local tumor was based on extent and organ confinement. Pelvic node metastases were categorized as single involved nodal regions (miN1a) or multiple involved nodal regions. Distant metastases were classified as extrapelvic lymph nodes (miM1a), bone metastases (miM1b), or organ metastases (miM1c). Bone disease was subcategorized as unifocal, oligometastatic, disseminated, or diffuse marrow involvement (oligometastatic bone involvement was interpreted as present when there were a maximum of 3 bone lesions) (15).  $\text{SUV}_{\text{max}}$  was calculated as a measure of PSMA expression.

**TABLE 2**  
Patient Characteristics (*n* = 200)

Characteristic	Frequency	Mean ± SD	Median	Interquartile range
Age (y)		69 ± 8	70	64–74
Weight (kg)		80 ± 11	79	72–87
BMI		26.7 ± 4	26.2	24.0–29.0
Injected activity (MBq)		160 ± 21	157	150–174
Uptake time (min)		73 ± 13	70	65–82
PSA PET (ng/mL)		10.4 ± 72.9	0.9	0.4–2.2
Clinical indication				
Primary staging	7/200 (4%)			
Biochemical recurrence	168/200 (84%)			
Castration-resistant PCa	25/200 (12%)			
PET device				
Discovery 710	78/200 (39%)			
Discovery STE	122/200 (61%)			

### Quality Assessment

For quality assessment, 2 other senior nuclear medicine physicians, highly experienced in PCa imaging and with at least 2 y of PSMA imaging practice, independently reviewed all 200 PSMA-PET images. Neither physician was aware of the individual clinical history or the used synthesis procedure (synthesis module or cold kit). They subjectively assessed the perceived quality of the image. Half of the final score was based on 5 quality parameters: optical texture (smoothness vs. graininess of liver uptake), sharpness (vs. blur) at sites of physiologic uptake, image detail, image contour rendering, and perceived image quality in terms of lesion detection. The remaining half was based on the presence or absence of artifacts in the scatter-corrected images, with particular focus on the presence of the halo artifact, defined as areas of artificially reduced, apparent tracer uptake near structures with intense PSMA uptake (especially the kidneys and bladder). After final scoring, the included imaging datasets were subgrouped according to a 3-point Likert scale for quality level (excellent, good, or moderate). Regions of interest were drawn around pathologic foci, and  $SUV_{max}$  was obtained for the most relevant lesions. In cases of discordance, the operators reviewed the images and reached a consensus. Figures 1 and 2 compare 2  $^{68}\text{Ga}$ -PSMA-11 PET/CT acquisitions rated as of good and moderate quality, respectively, using different production procedures.

### Statistical Analysis

For continuous data, we report mean ± SD, median, and interquartile range, whereas categorical variables are described using absolute and relative (%) frequencies. Associations between image quality and categorical variables were evaluated with the Pearson  $\chi^2$  test, whereas ANOVA was used for continuous variables (age, weight, BMI, injected dose, time of uptake). Because of an extremely asymmetric distribution of PSA, its association with image quality was assessed with the nonparametric Kruskal–Wallis test. Finally, significant variables were entered into a multiple logistic regression model to identify independent factors associated with a not-excellent image quality. For this purpose, the image quality evaluation was dichotomized into excellent versus not excellent (good plus moderate) judgment. To avoid collinearity between weight and BMI, only weight was considered in the model. Model goodness of fit was evaluated with the test of Hosmer and Lemeshow. Statistical analysis was conducted with Stata statistical software, version 13 (StataCorp), and a *P* value lower than 0.05 was considered significant.

## RESULTS

### Patient Population Characteristics

Among the 200 patients, median age was 70 y (interquartile range, 64–74 y) and median serum PSA level at the time of PSMA-PET was 0.9 ng/mL (interquartile range, 0.4–2.2 ng/mL). Regarding the PCa indication, 7 of the 200 (4%) PET referrals were for primary staging, 168 (84%) were for restaging during biochemical recurrence, and 25 (12%) were for restaging due to castration resistance. Complete clinical data are reported in detail in Table 2. Patient weight averaged  $79.8 \pm 11.5$  kg (range, 54–155 kg). The average BMI was  $26.7 \pm 3.7$ . None of the patients experienced immediate adverse reactions relating to the procedure.

### $^{68}\text{Ga}$ -PSMA-11 Preparation and Quality Control

The synthesis yield with the automatic module was more than 80%, corrected for the decay in 20 min. Radiochemical purity was more than 98%, and ethanol and residual  $^{68}\text{Ge}$  content complied with European Pharmacopoeia specifications. The product was sterile and nonpyrogenic. The synthesis yield with the cold kit was 99.9%, corrected for decay (all  $^{68}\text{Ga}$  activity coming from the generator was available as radiopharmaceutical). Radiochemical purity was more than 98%, and the product was found to be ethanol-free, sterile, and nonpyrogenic. The residual content of  $^{68}\text{Ge}$  complied with the specifications of the European Pharmacopoeia.

### Image Interpretation

The  $^{68}\text{Ga}$ -PSMA-11 PET/CT images were positive in 103 of the 200 patients, resulting in an overall positivity rate of 52%. Local

**TABLE 3**  
Association Between  $^{68}\text{Ga}$ -PSMA-11 Production and Image Quality

Association	Module	Kit	Total
Excellent	34	45	79 (39.5%)
Good	49	46	95 (47.5%)
Moderate	17	9	26 (13.0%)
Total	100	100	200



**TABLE 4**  
Logistic Regression Model Estimations for Presence of Poor Image Quality

Characteristic	Simple logistic model			Multivariable logistic model		
	OR	95% CI	<i>P</i>	OR	95% CI	<i>P</i>
Age (5-y increase)	1.25	1.04–1.50	0.015	1.40	1.12–1.75	0.003
Weight (5-kg increase)	1.63	1.37–1.94	<0.001	1.89	1.53–2.32	<0.001
Uptake time (10-min increase)	1.40	1.09–1.80	0.008	1.45	1.08–1.96	0.013
Injected activity (10-MBq decrease)	1.20	1.04–1.38	0.013	1.28	1.07–1.52	0.006

recurrence within the pelvis was reported for 26% (52/200) of patients, and distant metastases were identified in 26% (51/200). All identified pathologic foci corresponded to anatomic abnormalities on CT. In detail, 30 pathologic lesions (15%) were localized on the prostate gland/bed site (T/Tr), and SUV<sub>max</sub> ranged from 3.1 to 27.9. Forty-one patients (21%) had pathologic pelvic nodes (N1), with an SUV<sub>max</sub> ranging from 2.2 to 47.8. Twenty-two (11%) patients showed distant lymph node involvement (M1a), with an SUV<sub>max</sub> ranging from 3.3 to 50.5. Thirty-seven (19%) patients showed bone involvement (M1b), with an SUV<sub>max</sub> ranging from 1.9 to 43.0. In 4 patients (2%), PSMA-PET detected visceral metastases (M1c): 2 in the lungs and 2 in the liver; the recorded SUV<sub>max</sub> was 15.9.

#### Image Quality and Association with Patient Characteristics

Both operators considered all examinations as diagnostic. In cases of discordance, the operators reviewed the images and reached a consensus. The 2 operators rated 79 images (39.5%) as excellent, 95 (47.5%) as good, and 26 (13%) as moderate (Table 3). Fifty patients (25%) showed the presence of artifacts (Fig. 3): 15 within the kit group (15%) and 35 within the module group (35%). Three patients (1.5%) had blood extravasation at the injection site (commonly brachial). There was no significant difference in the ratings between kits and modules (*P* = 0.13), although the percentage of images rated as excellent was higher in the kit group (45% vs. 34%) (Table 3). A direct comparison was made of the novel cold kit-based <sup>68</sup>Ga-PSMA-11 with the clinically established module-based <sup>68</sup>Ga-PSMA-11 in patients of the same PCa cohort, in particular the biochemically recurrent group (168 patients). We found no significant difference in image quality between kit and cassette (*P* = 0.344); the percentage of excellent images was higher in the kit group than the cassette group (43.5% vs. 31.1%). There were also no significant differences between production modalities in the overall report conclusions (in terms of presence or absence of pathologic uptake).

Regarding patient characteristics, correlation with age was statistically significant (*P* = 0.04). Within the group for which images were rated as excellent, age was on average lower. However, when modular and kit synthetic protocols were considered separately, in the former group there was a directly proportional correspondence between increase in age and decrease in image quality, and the difference between the 3 levels (excellent, moderate, and poor) was statistically significant (*P* = 0.03). However, in the latter group of patients (cold kit), the association between image quality and age was not significant. Clearer, significant correlations were, on the other hand, found between overall image quality and other variables such as weight, BMI, and uptake time (*P* < 0.01). The higher those 3 parameters were, the lower the image quality was, regardless of the used production system, although when the cold kit was in use, variability in uptake time was found to be less relevant.

Moreover, the increase in injected activity was significantly related to better image quality (*P* = 0.02), although when modular and kit synthetic protocols were considered separately, the association was significant only in the latter. Conversely, serum PSA levels, as well as the used PET/CT system, had no significant impact on image quality. Furthermore, after image quality had been dichotomized as excellent or not excellent, multivariate regression analysis found several factors to be significantly associated with a not-excellent quality: an increase in patient age (+5 y: odds ratio [OR], 1.40; 95% confidence interval [CI], 1.12–1.75), an increase in patient weight (+5 kg: OR, 1.89; 95% CI, 1.53–2.32), an increase in <sup>68</sup>Ga-PSMA-11 uptake time (+10 min: OR, 1.45; 95% CI, 1.08–1.96), and a decrease in injected activity (–10 MBq: OR, 1.28; 95% CI, 1.07–1.52).

#### DISCUSSION

Our retrospective analysis comparing 2 different cohorts of heterogeneous PCa patients showed no statistically significant difference in PSMA-PET image quality (*P* = 0.18). Nevertheless, the percentage of images rated as excellent was slightly higher in

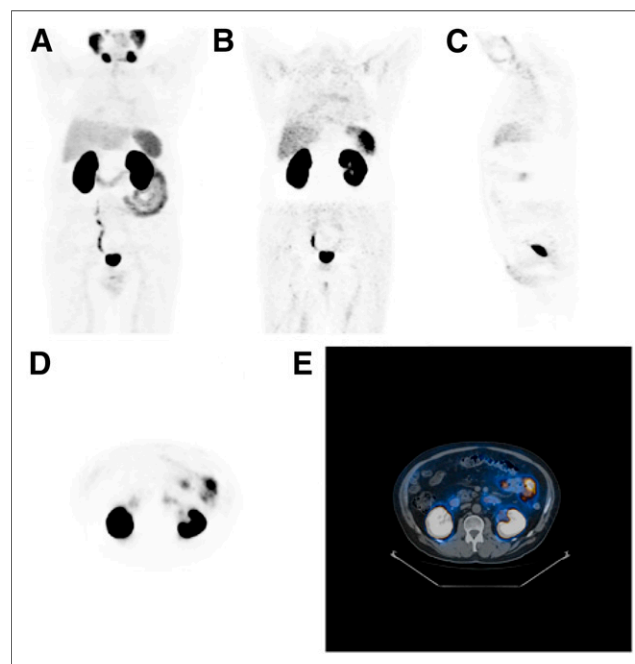


**FIGURE 3.** Presence of halo artifact on PET/CT images around kidneys on <sup>68</sup>Ga-PSMA-11 PET/CT. Shown are maximum-intensity projection (A), coronal PET (B), sagittal PET (C), axial PET (D), and PET/CT (E) of abdomen at level of kidneys, with high urinary tracer activity causing artifact.

**TABLE 5**  
Main Advantages and Disadvantages of Automated Synthesis Module vs. Kit

<sup>68</sup> Ga-PSMA-11 preparation	Synthesis module	Kit
Yield (%) corrected for decay	>80	99.9*
Time of synthesis (min)	20	10
<sup>68</sup> Ga/ <sup>68</sup> Ge eluate and product purification	Need to elute and purify product	No need to elute and purify product
Preparation of reagents before synthesis	Need to prepare cassette and reagents	All necessary materials are provided with kit
Installation and maintenance issues	Need to install and maintain module	No need to install and maintain module
Operational complexity	Need to train staff	Need to train staff, but less operational complexity
Radiochemical purity (%)	>98	>98
<sup>68</sup> Ge content (%)	0.00001	0.0001
Ethanol content	Complied with European Pharmacopoeia specifications	Not present
Sterility and pyrogen content	Complied with European Pharmacopoeia specifications	Complied with European Pharmacopoeia specifications

\*All <sup>68</sup>Ga activity from generator available as radiopharmaceutical.

the kit group than the module group, possibly because of a lower percentage of halo artifacts in the former (15% vs. 35%). Thus, the type of <sup>68</sup>Ga-PSMA-11 synthesis procedure applied, either modular or a cold kit, did not influence image assessment. Nevertheless, factors impactful on PSMA-PET image quality were found to be patient weight, patient age, and uptake time. For higher values of these 3 parameters, the image quality worsened, regardless of the production method used. There was no significant association between image quality and <sup>68</sup>Ga-PSMA-11 injected activity in a setting where we administered 1.8–2.2 MBq of tracer per kilogram of body weight, in compliance with the European Association of Nuclear Medicine procedure guidelines, with injected activities under no circumstances falling below 50 MBq per patient; individual PET/CT; and serum PSA levels at the time of the scan. However, only a few scans were rated as moderate in quality, and none was judged so poor as to be described as nondiagnostic.

Traditionally, <sup>68</sup>Ga-PSMA-11 can be prepared using a <sup>68</sup>Ge/<sup>68</sup>Ga generator and a manual synthesis module. Nanabala et al. previously studied its stability and radiochemical purity, and the product was found to be extraordinarily stable, ensuring at the same time a high standard of radiologic safety for the operator. In addition, the generator and the modules can be operated several times a day, the production of the radiopharmaceutical is relatively simple and economical, and it can be performed by an expert technologist (16). However, several studies are currently supporting the feasibility and operational safety of a new radiopharmaceutical, tris(hydroxypyridinone) (THP)-PSMA, labeled in a single step with cold reconstitution by means of a kit. In particular, in a phase I study comparing one cohort receiving PSMA-11 and another receiving THP-PSMA, Hofman et al. demonstrated that THP-PSMA is safe and has a favorable biodistribution for clinical imaging (17). Moreover, Derlin et al., in a retrospective study, found suitable in vivo uptake characteristics for THP-PSMA (kit-based) and suggested the feasibility of its wider application, with a higher patient throughput (18).

Our data support the hypothesis that <sup>68</sup>Ga-PSMA-11 cold kit production may be a promising tool, as previously suggested by Beheshti et al. (12), without a detrimental effect on image quality in everyday clinical routine. Kit formulations may allow for local, on-demand production, overcoming the issues posed by the complexity of synthetic procedures while resulting in higher yields with a standardized, high degree of radiochemical purity. Additionally, in situations of high demand, using kits may free all generator-based <sup>68</sup>Ga activity for modular synthesis, significantly increasing the available radiopharmaceuticals on a daily basis, with a comparable degree of radiochemical purity among all injected tracers. A <sup>68</sup>Ga-PSMA-11 cold kit may easily be implemented in a clinical radiopharmacy, the main advantages being less operational complexity, no installation or maintenance costs, and no need for additional staff training or for additional reagents. Furthermore, using a kit might significantly speed production, cutting operational time (no need for module and reagent preparation, no generator eluate, and no product purification) and overall costs, thus making the sterile cold kit a valid alternative to the synthesis module for the preparation of <sup>68</sup>Ga-PSMA-11 in clinical practice.

Table 5 shows the main advantages and disadvantages of automated synthesis module production versus kit-based <sup>68</sup>Ga-PSMA-11 production. Although our results seem to support the above conclusions, our study suffers from a few limitations, including its retrospective design, a suboptimal agreement between 2 independent readers, and the heterogeneity of our cohorts of patients, who had different stages of prostate disease.

## CONCLUSION

No significant differences in PET/CT image quality were found between <sup>68</sup>Ga-PSMA-11 synthesized using a cold kit and <sup>68</sup>Ga-PSMA-11 synthesized using a module, in 2 separate groups of PCa patients. Factors significantly associated with a not-excellent image quality included an increase in patient age, an increase in

patient weight, a decrease in injected activity, and an increase in  $^{68}\text{Ga}$ -PSMA-11 uptake time. Our results suggest that cold kit synthesis of  $^{68}\text{Ga}$ -PSMA-11 may successfully be implemented for the imaging of PCa patients.

## DISCLOSURE

Cold kits were provided free of charge by ANMI SA, Liège, Belgium. No other potential conflict of interest relevant to this article was reported.

## KEY POINTS

**QUESTION:** Are there significant differences between different synthesis procedures in term of final image quality in  $^{68}\text{Ga}$ -PSMA-11 PET/CT?

**PERTINENT FINDINGS:** In this retrospective single-center cohort study comparing 2 groups of 100 patients each, no significant differences were found in terms of image quality between the 2 groups.

**IMPLICATIONS FOR PATIENT CARE:** Although comparable in quality to standard procedures, kit-based synthesis may allow for a more widespread diffusion of PSMA-ligand PET imaging.

## REFERENCES

1. Ferlay J, Soerjomataram I, Dikshit R, et al. Cancer incidence and mortality worldwide: sources, methods and major patterns in GLOBOCAN 2012. *Int J Cancer*. 2015;136:E359–E386.
2. Perera M, Papa N, Christidis D, et al. Sensitivity, specificity, and predictors of positive  $^{68}\text{Ga}$ -prostate-specific membrane antigen positron emission tomography in advanced prostate cancer: a systematic review and meta-analysis. *Eur Urol*. 2016;70:926–937.
3. Eiber M, Maurer T, Souvatzoglou M, et al. Evaluation of hybrid  $^{68}\text{Ga}$ -PSMA ligand PET/CT in 248 patients with biochemical recurrence after radical prostatectomy. *J Nucl Med*. 2015;56:668–674.
4. Rauscher I, Maurer T, Beer AJ, et al. Value of  $^{68}\text{Ga}$ -PSMA HBED-CC PET for the assessment of lymph node metastases in prostate cancer patients with biochemical recurrence: comparison with histopathology after salvage lymphadenectomy. *J Nucl Med*. 2016;57:1713–1719.
5. Eder M, Schäfer M, Bauder-Wüst U, et al.  $^{68}\text{Ga}$ -complex lipophilicity and the targeting property of a urea-based PSMA inhibitor for PET imaging. *Bioconjug Chem*. 2012;23:688–697.
6. Afshar-Oromieh A, Haberkorn U, Eder M, Eisenhut M, Zechmann CM. [ $^{68}\text{Ga}$ ]gallium-labelled PSMA ligand as superior PET tracer for the diagnosis of prostate cancer: comparison with  $^{18}\text{F}$ -FECH. *Eur J Nucl Med Mol Imaging*. 2012;39:1085–1086.
7. Weineisen M, Schottelius M, Simecek J, et al.  $^{68}\text{Ga}$ - and  $^{177}\text{Lu}$ -labeled PSMA I&T: optimization of a PSMA-targeted theranostic concept and first proof-of-concept human studies. *J Nucl Med*. 2015;56:1169–1176.
8. Afshar-Oromieh A, Malcher A, Eder M, et al. PET imaging with a [ $^{68}\text{Ga}$ ]gallium-labelled PSMA ligand for the diagnosis of prostate cancer: biodistribution in humans and first evaluation of tumour lesions. *Eur J Nucl Med Mol Imaging*. 2013;40:486–495.
9. Cho SY, Gage KL, Mease RC, et al. Biodistribution, tumor detection, and radiation dosimetry of  $^{18}\text{F}$ -DCFBC, a low-molecular-weight inhibitor of prostate-specific membrane antigen, in patients with metastatic prostate cancer. *J Nucl Med*. 2012;53:1883–1891.
10. Chen Y, Pullambhatla M, Foss CA, et al. 2-(3-{1-carboxy-5-[(6-[ $^{18}\text{F}$ ]fluoropyridine-3-carbonyl)-amino]-pentyl}-ureido)-pentanedioic acid, [ $^{18}\text{F}$ ]DCFpYL, a PSMA-based PET imaging agent for prostate cancer. *Clin Cancer Res*. 2011;17:7645–7653.
11. Cardinale J, Schäfer M, Benešová M, et al. Preclinical evaluation of  $^{18}\text{F}$ -PSMA-1007, a new prostate-specific membrane antigen ligand for prostate cancer imaging. *J Nucl Med*. 2017;58:425–431.
12. Beheshti M, Paymani Z, Brillhante J, et al. Optimal time-point for  $^{68}\text{Ga}$ -PSMA-11 PET/CT imaging in assessment of prostate cancer: feasibility of sterile cold-kit tracer preparation? *Eur J Nucl Med Mol Imaging*. 2018;45:1188–1196.
13. Eder M, Neels O, Müller M, et al. Novel preclinical and radiopharmaceutical aspects of [ $^{68}\text{Ga}$ ]Ga-PSMA-HBED-CC: a new PET tracer for imaging of prostate cancer. *Pharmaceuticals (Basel)*. 2014;7:779–796.
14. Fendler WP, Eiber M, Beheshti M, et al.  $^{68}\text{Ga}$ -PSMA PET/CT: joint EANM and SNMMI procedure guideline for prostate cancer imaging: version 1.0. *Eur J Nucl Med Mol Imaging*. 2017;44:1014–1024.
15. Eiber M, Herrmann K, Calais J, et al. Prostate cancer molecular imaging standardized evaluation (PROMISE): proposed miTNM classification for the interpretation of PSMA-ligand PET/CT. *J Nucl Med*. 2018;59:469–478.
16. Nanabala R, Anees MK, Sasikumar A, Joy A, Pillai MRA. Preparation of [ $^{68}\text{Ga}$ ]PSMA-11 for PET-CT imaging using a manual synthesis module and organic matrix based  $^{68}\text{Ge}/^{68}\text{Ga}$  generator. *Nucl Med Biol*. 2016;43:463–469.
17. Hofman MS, Eu P, Jackson P, et al. Cold kit for prostate-specific membrane antigen (PSMA) PET imaging: phase 1 study of  $^{68}\text{Ga}$ -tris(hydroxypyridinone)-PSMA PET/CT in patients with prostate cancer. *J Nucl Med*. 2018;59:625–631.
18. Derlin T, Schmuck S, Juhl C, et al. PSA-stratified detection rates for [ $^{68}\text{Ga}$ ]THP-PSMA, a novel probe for rapid kit-based  $^{68}\text{Ga}$ -labeling and PET imaging, in patients with biochemical recurrence after primary therapy for prostate cancer. *Eur J Nucl Med Mol Imaging*. 2018;45:913–922.